

## Study of the ${}^6\text{Li}({}^6\text{Li}, {}^6\text{Li}^*(3.56)){}^6\text{Li}^*(3.56)$ and the ${}^6\text{Li}({}^6\text{Li}, {}^6\text{He}){}^6\text{Be}$ reactions\*

W. R. Wharton,<sup>†</sup> J. G. Cramer, J. R. Calarco,<sup>‡</sup> and K. G. Nair

*Department of Physics, University of Washington, Seattle, Washington 98195*

(Received 13 July 1973)

Angular distributions have been measured for the  ${}^6\text{Li}({}^6\text{Li}, {}^6\text{Li}^*(3.56)){}^6\text{Li}^*(3.56)$  and the  ${}^6\text{Li}({}^6\text{Li}, {}^6\text{He}){}^6\text{Be}$  reactions at laboratory bombarding energies of 32 and 36 MeV, and excitation functions have been measured at 88° in the center of mass. All final-state nuclei are members of the same  $T=1$  isomultiplet and according to charge independence, the two reactions should have equal cross sections. Large differences in the cross sections of the two reactions are observed indicating that charge-dependent effects are important. For example at 32 MeV the ratio of the two cross sections,  ${}^6\text{Li}({}^6\text{Li}, {}^6\text{Li}^*){}^6\text{Li}^*/{}^6\text{Li}({}^6\text{Li}, {}^6\text{He}){}^6\text{Be}$ , oscillates with angle, varying in magnitude from 0.17 to greater than 1.65.

NUCLEAR REACTIONS  ${}^6\text{Li}({}^6\text{Li}, {}^6\text{Li}^*(3.56)), ({}^6\text{Li}, {}^6\text{He}), E=28-36$  MeV; measured  $\sigma(E, \theta)$ ,  $\theta=17-90^\circ$  c.m.,  $\Delta\theta=4^\circ$ ; Legendre polynomial expansion of  $\sigma(\theta)$ .

Reactions of the type  $({}^6\text{Li}, {}^6\text{He})$  and  $({}^6\text{Li}, {}^6\text{Li}^*)$ , where  ${}^6\text{Li}^*$  refers specifically to the  $0^+$  state at 3.56 MeV excitation in  ${}^6\text{Li}$ , have been characterized as quasielastic double-spin-isospin-flip reactions.<sup>1-3</sup> This "quasielastic" process is defined as one valence nucleon in the  ${}^6\text{Li}$  projectile interacting directly with a single nucleon in the target nucleus causing a spin and isospin reorientation of each nucleon. The  ${}^6\text{Li}^*(3.56)$  and  ${}^6\text{He}$  ground state have nearly the same configuration<sup>4</sup> as the  ${}^6\text{Li}$  ground state except for the spin-isospin reorientation of a  $1p$ -shell nucleon. Therefore the  $(\vec{\sigma}_i \cdot \vec{\sigma}_j)(\vec{\tau}_i \cdot \vec{\tau}_j)$  term of the effective nucleon-nucleon potential may cause such a double-spin-isospin flip. Because of the small quantity and poor quality of the data accumulated on the  $({}^6\text{Li}, {}^6\text{He})$  and  $({}^6\text{Li}, {}^6\text{Li}^*)$  reactions, the quasielastic description of the reaction process has not been adequately proven.

In this report an accurate comparison of the  ${}^6\text{Li}({}^6\text{Li}, {}^6\text{Li}^*){}^6\text{Li}^*$  and the  ${}^6\text{Li}({}^6\text{Li}, {}^6\text{He}){}^6\text{Be}$  cross sections is made with measurements of angular distributions at bombarding energies of 32 and 36 MeV and excitation functions near 90° in the center of mass. The three final states,  ${}^6\text{He}$ ,  ${}^6\text{Li}^*(3.56)$ , and  ${}^6\text{Be}$  are members of the same  $T=1$  isomultiplet, and if charge independence is valid the cross sections of the two reactions must be equal. However, there are several charge-dependent effects in these reactions which cause the cross sections to be nonequal. For example, it is known that electromagnetic forces, among other things, affect the binding energy of the final nuclei so that the  ${}^6\text{Be}$  is unbound by 1.37 MeV to  $\alpha+2p$  decay and  ${}^6\text{Li}^*(3.56)$  and  ${}^6\text{He}$  are particle stable. This further leads to different  $Q$  values which are -7.12 MeV for the  ${}^6\text{Li}({}^6\text{Li}, {}^6\text{Li}^*){}^6\text{Li}^*$  reaction and

-7.89 MeV for the  ${}^6\text{Li}({}^6\text{Li}, {}^6\text{He}){}^6\text{Be}$  reaction. The effect that the charge dependence has upon the cross sections will depend partially upon the reaction mechanism. Therefore measured differences in the cross sections for the two reactions can be used as additional information to study the extent that the reaction is quasielastic. Alternatively, if the reaction is known to be quasielastic, differences in the cross sections for the two reactions can be used to study differences in the wave functions of the isomultiplet.

This report has been separated into two parts. The first part presented here, is primarily a presentation of the data. The second part, which appears in a subsequent publication,<sup>5</sup> is a partial microscopic distorted-wave Born-approximation (DWBA) analysis of the data to study the reaction mechanism, charge independence, and the effective nucleon-nucleon interaction.

### MEASUREMENT PROCEDURE

The  ${}^6\text{Li}({}^6\text{Li}, {}^6\text{Li}^*){}^6\text{Li}^*$  reaction has been measured previously<sup>2</sup> by detecting the two  ${}^6\text{Li}^*$  nuclei in coincidence using detectors of equal solid angle. The coincidence is necessary to distinguish the  ${}^6\text{Li}({}^6\text{Li}, {}^6\text{Li}^*){}^6\text{Li}^*$  reaction from three-body final states, but the equality of the detector solid angles in that experiment resulted in poor coincidence efficiency and correspondingly large uncertainties in the cross sections. In the present experiment, the coincidence efficiency has been improved by making the solid angle of one of the detectors up to 1000 times the solid angle of the other detector ( $5 \times 10^{-2}$  sr vs  $5 \times 10^{-5}$  sr). With each  ${}^6\text{Li}$  detected in the smaller detector, the corresponding  ${}^6\text{Li}$  recoil will nearly always be detected in the large de-

tor, resulting in nearly 100% efficiency.

It is advantageous to measure the  ${}^6\text{Li}({}^6\text{Li}, {}^6\text{Li}^*)$ - ${}^6\text{Li}^*$  and  ${}^6\text{Li}({}^6\text{Li}, {}^6\text{He}){}^6\text{Be}$  reactions simultaneously in the same detector because then a direct comparison of the two cross sections can be made nearly independent of the target thickness, the integrated beam on target, or the detector solid angle. No analogous coincidence requirement can be used for the  ${}^6\text{Li}({}^6\text{Li}, {}^6\text{He}){}^6\text{Be}$  reaction because  ${}^6\text{Be}$  is particle unstable. The smaller of the two detectors is chosen to be the  $\Delta E$ - $E$  telescope for identifying the  ${}^6\text{Li}$  and  ${}^6\text{He}$  nuclei. The larger detector is placed to detect the recoil  ${}^6\text{Li}$  ions. All these detectors are surface-barrier detectors. An anticoincidence detector is placed behind the  $E$  detector to reject all particles not stopped in the telescope. Standard electronics are used in this experiment.

The experimental data is collected on-line in the University of Washington SDS 930 computer. A standard laboratory data collection program<sup>6</sup>

which calculates particle identification from the  $\Delta E$  and  $E$  energy signals was altered specifically for this experiment. Briefly the program calculates the particle identification from the  $\Delta E$  and  $E$  energy signals and displays the particle identification spectrum, as shown on Fig.1 (a). The experimenter sets windows on three areas of the spectrum of which two include the  ${}^6\text{He}$  and  ${}^6\text{Li}$  particle peaks. Events falling within each window are stored in separate bins and the energy spectra of each bin are displayed over 1024 channels. Events falling within the  ${}^6\text{Li}$  window are further separated according to whether they are in coincidence or not in coincidence with a fast-timing logic signal which enters the computer through a third analog-to-digital converter (ADC). Typical  ${}^6\text{He}$ ,  ${}^6\text{Li}$  coincidence, and  ${}^6\text{Li}$  noncoincidence spectra are shown in Fig. 1(b). As is seen, the coincidence is required to reduce the background under the  ${}^6\text{Li}({}^6\text{Li}, {}^6\text{Li}^*){}^6\text{Li}^*$  peak in order to observe the peak.

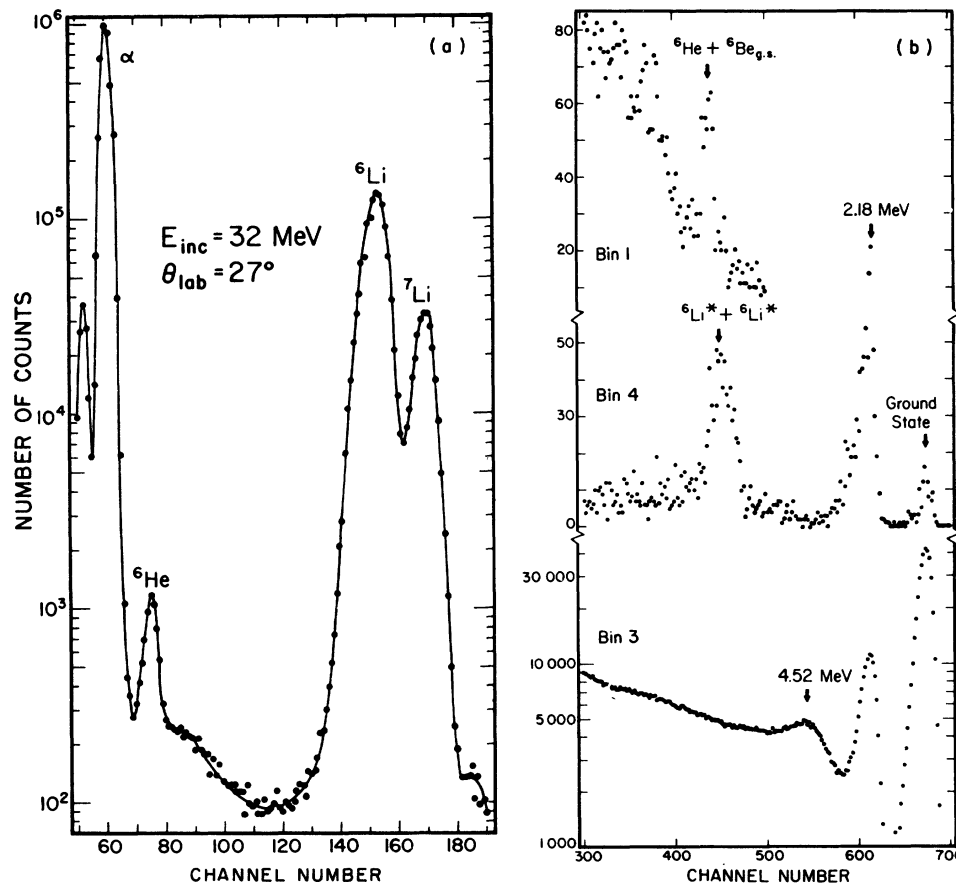


FIG. 1. The spectra of a run at  $E_{\text{lab}} = 32 \text{ MeV}$  and  $\theta_{\text{lab}} = 27^\circ$ . Windows are set on the  ${}^6\text{He}$  and  ${}^6\text{Li}$  peaks of the particle identification spectrum (a) and the energy spectra (b) are stored for each window. The windows are: Bin 1 includes channels 69–87, Bin 4 includes channels 137–163 with coincidences, and Bin 3 includes channels 137–163 without coincidences.

The computer stores the array of numbers,  $I^x$ , for all integers  $I$  up to a sufficiently high number, and using this stored array calculates the particle identification, I.D., according to the relation

$$\text{I.D.} = C[\Delta E + E + IS]^x - (E + IS)^x, \quad (1)$$

where  $C$ ,  $IS$ , and  $x$  are adjustable parameters. Equation (1) is easily derivable from an empirical range-energy relationship

$$R = a(E + IS)^x, \quad (2)$$

$$\text{I.D.} = t/a, \quad (3)$$

where  $R$  is the range of a particle with energy  $E$ ,  $a$  is a constant which is dependent upon the mass and the charge of the particle, and  $t$  is the thickness of the  $\Delta E$  detector. The only difference between the empirical formulas (1) and (2) and the more standard formulas is the inclusion of the parameter  $IS$ . We found that the inclusion of  $IS$  greatly improves<sup>7</sup> the fit of the empirical formula (2) to the range-energy tables of Northcliffe and Schilling.<sup>8</sup> Experimentally we find that with  $IS \approx 3.0$  MeV, the peak-to-valley ratio for the  ${}^6\text{He}$  peak is a factor 1.5 better than with  $IS=0$ . This means that there is at least 50% less  ${}^4\text{He}$  feed-through into our  ${}^6\text{He}$  energy spectrum as a result of including  $IS$  as an additional parameter. With  $IS=3$  MeV, the best value of  $x$  is about 1.78.

A separate monitor detector for normalizing measurements at different angles is not necessary since we use the elastic scattering data which is recorded simultaneously in the computer along with events from the  ${}^6\text{Li}({}^6\text{Li}, {}^6\text{Li}^*){}^6\text{Li}^*$  and the  ${}^6\text{Li}({}^6\text{Li}, {}^6\text{He}){}^6\text{Be}$  reactions. All cross sections are normalized to the elastic scattering data which serves as a monitor. The elastic scattering cross sections are measured separately using a separate monitor detector and the absolute cross sections are obtained by normalizing the data points at  $E_{\text{lab}} = 32$  MeV,  $\theta_{\text{lab}} = 90, 80, 70,$  and  $60^\circ$  with the excitation functions of Fortune, Morrison, and Siemssen<sup>9</sup> for which the absolute cross sections were determined to within 5% error.

Although the coincidence efficiency is greatly improved by choosing a large solid angle for the recoil detector, there are still losses of  ${}^6\text{Li}({}^6\text{Li}, {}^6\text{Li}^*){}^6\text{Li}^*$  events due to the coincidence requirement. If the  ${}^6\text{Li}({}^6\text{Li}, {}^6\text{Li}^*){}^6\text{Li}^*$  and the  ${}^6\text{Li}({}^6\text{Li}, {}^6\text{He}){}^6\text{Be}$  cross sections are to be accurately compared, these losses must be determined and corrected for. Most of the losses occur when the telescope is at forward angles and the recoil  ${}^6\text{Li}$  has very little kinetic energy. In this situation multiple scattering of the recoil  ${}^6\text{Li}^*$  in the target becomes very important and the angular deflection of each  ${}^6\text{Li}^*$  due to its photon decay also becomes impor-

tant. To compound the problem, there are large kinematic magnification factors at forward angles which increase the uncertainty of the angular correlation between the scattering angle of the ion detected in the telescope and the scattering angle of the recoil ion. These magnification factors were as large as 4.73 for some measurements.

During the measurements for which multiple scattering in the target is important, we use the thinnest available  ${}^6\text{Li}$  foil. The targets are self-supported isotopically enriched  ${}^6\text{Li}$  foils varying in thickness from 80 to 300  $\mu\text{g}/\text{cm}^2$  and made by the vacuum evaporation technique.<sup>10</sup> Even with 80- $\mu\text{g}/\text{cm}^2$  targets, the root-mean-squared multiple scattering angle,  $\bar{\theta}_{\text{ms}}$ , is larger than  $4^\circ$  for the lowest-energy  ${}^6\text{Li}$  ions. The multiple-scattering angle has an approximately Gaussian distribution.<sup>11</sup> Both the importance of the multiple scattering and the goodness of the in-plane alignment are observed by measuring angular correlations on the elastically scattered lithium nuclei. Misalignment occurs when the target becomes warped. The cause of warping is oxidation, and therefore special precaution has to be taken to avoid contact of the target with air.

To determine the coincidence efficiency for the  ${}^6\text{Li}({}^6\text{Li}, {}^6\text{Li}^*){}^6\text{Li}^*$  reaction, the data collection follows certain specific procedures. First, the elastic coincidence efficiency is measured with the angles of the detectors chosen so that the elastic recoil has the same energy that the inelastic recoil is to have in the following measurement. The recoil energies are chosen equal so that we can accurately monitor the multiple scattering in the target and set an electronic discriminator level to reject recoil ions below a certain energy. After the elastic coincidence efficiency is accurately measured by recording the elastic events in the  ${}^6\text{Li}$ -coincidence and  ${}^6\text{Li}$ -noncoincidence spectra, the angles of the detectors are changed to measure the  ${}^6\text{Li}({}^6\text{Li}, {}^6\text{Li}^*){}^6\text{Li}^*$  reaction. Each measurement lasts from 4 to 12 h, and to verify that nothing has changed during this long time, the elastic coincidence efficiency is again measured after each  ${}^6\text{Li}({}^6\text{Li}, {}^6\text{Li}^*){}^6\text{Li}^*$  measurement is completed. In only one instance has the efficiency significantly changed and in that case the whole measurement was rejected.

#### EFFICIENCY CALCULATIONS

The coincidence efficiency for the  ${}^6\text{Li}({}^6\text{Li}, {}^6\text{Li}^*){}^6\text{Li}^*$  reaction is calculated using the measured coincidence efficiency for the elastic scattering. The only differences between the two efficiencies result from differences in the kinematics and the photon decay of each  ${}^6\text{Li}^*$ . Both differences

can be calculated exactly. The  ${}^6\text{Li}^*(3.56)$  state is  $0^+$  and decays isotropically to the ground state.

For any  ${}^6\text{Li}$  nucleus which is detected in the telescope detector, the coincidence efficiency is the probability that the corresponding recoil  ${}^6\text{Li}$  is detected in the recoil detector (assuming no loss of events due to electronics). Two computer programs<sup>12</sup> have been written to calculate the elastic and inelastic coincidence efficiencies. The programs take the  ${}^6\text{Li}$  which is detected by the telescope, work backwards in time to the reaction and then forward in time with the recoil  ${}^6\text{Li}$ , determining its probability distribution over angle as it approaches the recoil detector. The probability function is integrated over the solid angle of the recoil detector to determine what fraction of the recoil  ${}^6\text{Li}$  is detected. The probability function is obtained by a mathematical folding procedure whereby the probability distribution due to each effect such as the finite solid angle of the telescope, the finite beam size on target, the multiple scattering of each  ${}^6\text{Li}$ , and the photon decay of each  ${}^6\text{Li}^*$  are folded into one another to obtain the complete probability distribution.

The procedure for obtaining the inelastic coincidence efficiencies is as follows. The elastic recoil probability distribution is adjusted to give the measured elastic coincidence efficiency. The adjustment is made by letting the root-mean-squared multiple scattering angle of the recoil  ${}^6\text{Li}$ ,  $\bar{\theta}_{ms}$ , be a free parameter since this is the least accurately known part of the whole calculation. The inelastic recoil probability distribution is obtained from the elastic recoil probability distribution by inserting the inelastic kinematic factors and including the effects of the photon decay of each  ${}^6\text{Li}^*$ . Integration of the inelastic recoil probability distribution over the solid angle of the recoil counter gives the inelastic efficiency.

The free adjustment of  $\bar{\theta}_{ms}$  not only takes care of the difficult problem of trying to solve for it, but it also crudely corrects for errors in the geometry and losses due to the electronics. For example, the calculations are performed assuming perfect alignment and then are carried through again assuming a misalignment of  $1^\circ$  for the position of the recoil detector. The two calculations give values of the inelastic coincidence efficiency which agree to within 0.3%. The reason the calculated inelastic efficiencies are nearly the same for both cases is that for a given geometry  $\bar{\theta}_{ms}$  adjusts itself to give the measured elastic efficiency. If there is a misalignment of  $1^\circ$  put into the geometry then  $\bar{\theta}_{ms}$  needs to be smaller to give the measured elastic efficiency. Both the misalignment and the smaller value of  $\bar{\theta}_{ms}$  carry over into the inelastic efficiency calculation and their

effects nearly cancel so that the calculated inelastic efficiency is nearly the same as when perfect alignment is assumed. For further details of these calculations see Ref. 12.

The calculated inelastic efficiencies vary between 70 and 99.9% and are greater than 90% at nearly all angles greater than  $20^\circ$  in the center of mass.

#### PEAK-SHAPE CALCULATIONS

The energy peak of the  ${}^6\text{Li}({}^6\text{Li}, {}^6\text{Li}^*){}^6\text{Li}^*$  reaction in the energy spectrum of the telescope detector is in some instances altered in shape by the efficiency losses. The experimental shape of the peak is additional information with which we can check the efficiency losses.

The energy peak of the  ${}^6\text{Li}({}^6\text{Li}, {}^6\text{Li}^*){}^6\text{Li}^*$  reaction is greatly broadened compared to the other peaks in the energy spectra. The reason for this is that the photon decay of the  ${}^6\text{Li}^*$  significantly changes its kinetic energy. The change in kinetic energy,  $E_s$ , is:

$$E_s = \frac{(\vec{P} - \vec{P}_\gamma)^2 - P^2}{2M_{\text{Li}}} \quad (4)$$

$$\cong \frac{-2PP_\gamma \cos \theta}{2M_{\text{Li}}} \quad \text{for } P \gg P_\gamma,$$

where  $\vec{P}$  is the momentum of the  ${}^6\text{Li}^*$ ,  $P_\gamma$  the momentum of the photon,  $M_{\text{Li}}$  the mass of Li, and  $\theta$  is the angle between  $\vec{P}$  and  $\vec{P}_\gamma$ . The photon decay is a 3.56-MeV transition to the ground state and if we include the Doppler shift but neglect the small recoil correction then:

$$P_\gamma = \frac{3.56}{(1 - \beta^2)^{1/2}} (1 + \beta \cos \theta) \text{ MeV}/c, \quad (5)$$

$$\beta = P/M_{\text{Li}}c.$$

Consider a specific example. The incident bombarding energy is 32 MeV and the  ${}^6\text{Li}^*$  is scattered at the angle  $\theta_{\text{lab}} = 8.9^\circ$  with a 23.57-MeV kinetic energy. In this case  $\beta = 0.09$  and

$$-350 \text{ keV} < E_s < 300 \text{ keV}. \quad (6)$$

The  ${}^6\text{Li}({}^6\text{Li}, {}^6\text{Li}^*){}^6\text{Li}^*$  energy peak is broadened by 650 keV and Doppler shifted downward by 25 keV. It can also be shown that the peak should be nearly flat on top (uniformly distributed over the 650-keV energy).

The experimental peak at  $8.9^\circ$  is measured to be 650 keV wide but the peak has a large dip at its center which is a result of lost coincidence events. The coincidence efficiency is calculated to be 82% and most of the lost events come from

the middle of the energy peak. The reason for this is that the middle of the energy peak corresponds to  $\cos\theta \approx 0$  which means the photon is coming off perpendicular to the direction of motion of the  ${}^6\text{Li}^*$  and is giving a large sideways deflection to the  ${}^6\text{Li}$  momentum. The result is that there are  ${}^6\text{Li}$  nuclei which would have missed the telescope which are deflected by the photon decay into the telescope detector. The recoil detector is then at the incorrect angle to catch the corresponding recoil  ${}^6\text{Li}$ . For this specific example, the error in the recoil angle is as large as  $1.68^\circ$ . Because the solid angle of the recoil detector is only  $10^{-2}$  sr for this measurement rather than  $5 \times 10^{-2}$  sr used in other measurements, the efficiency loss is more severe. The experimental energy peak and the calculations of its shape are shown in Fig. 2. The calculation with efficiency loss gives a dip in the middle of the peak which appears to be only half as deep as the experimental dip. The difference is probably statistical because all other energy peaks at other angles and energies show much smaller dips consistent with our calculations. For the energy peak in Fig. 2, the energy resolution is 150 keV. With this mediocre energy resolution and poor statistics, we conclude that the peak shapes cannot serve as a stringent test of our efficiency calculations, but that they do give some indication that we are doing the calculations correctly.

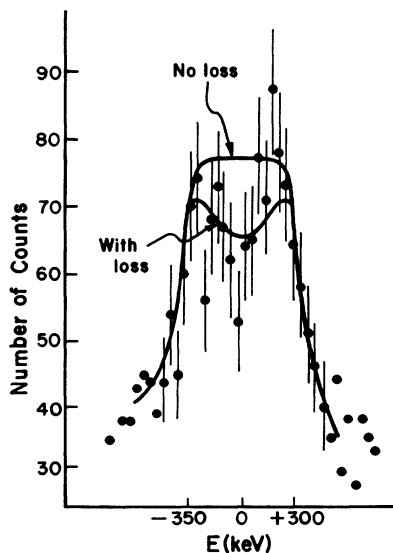


FIG. 2. The energy peak of the  ${}^6\text{Li}({}^6\text{Li}, {}^6\text{Li}^*(3.56)) - {}^6\text{Li}^*(3.56)$  reaction measured at  $E_{\text{lab}} = 32$  MeV and  $\theta_{\text{lab}} = 8.9^\circ$  in coincidence with the recoil  ${}^6\text{Li}$ . The calculations with coincidence loss or assuming no loss of events are shown by the labeled solid lines.

#### EXPERIMENTAL DATA

The  ${}^6\text{Li}({}^6\text{Li}, {}^6\text{Li}^*){}^6\text{Li}$  and  ${}^6\text{Li}({}^6\text{Li}, {}^6\text{He}){}^6\text{Be}$  angular distributions at bombarding energies of 32 and 36 MeV are shown in Fig. 3. The  ${}^6\text{Li}({}^6\text{Li}, {}^6\text{Li}^*){}^6\text{Li}^*$  measured cross sections have been corrected for efficiency loss. The two  ${}^6\text{Li}^*$  nuclei in the final state are identical and the experimental measurement of the differential cross section at the angle  $\theta$  in the center of mass will necessarily include the measurement of the differential cross section at the center-of-mass angle  $\pi - \theta$ ,

$$\frac{d\sigma_{\text{exp}}}{d\Omega} = \frac{d\sigma_{\text{c.m.}}(\theta)}{d\Omega} + \frac{d\sigma_{\text{c.m.}}(\pi - \theta)}{d\Omega} = \frac{2d\sigma_{\text{c.m.}}(\theta)}{d\Omega}. \quad (7)$$

The differential cross sections are symmetric about  $90^\circ$  because of the identity of the incident  ${}^6\text{Li}$  nuclei and to account for this double counting, we have divided the  ${}^6\text{Li}({}^6\text{Li}, {}^6\text{Li}^*){}^6\text{Li}^*$  experimental cross sections by 2. The errors include three

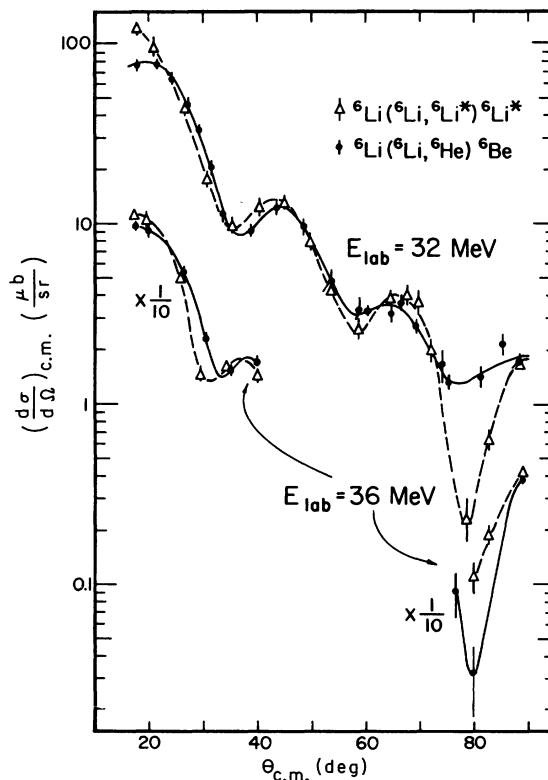


FIG. 3. Angular distributions for the  ${}^6\text{Li}({}^6\text{Li}, {}^6\text{Li}^*){}^6\text{Li}^*$  and the  ${}^6\text{Li}({}^6\text{Li}, {}^6\text{He}){}^6\text{Be}$  reactions at bombarding energies of 32 and 36 MeV are shown. At 32 MeV, they have been fit to an even Legendre polynomial expansion up to polynomials of order 16 for the  ${}^6\text{Li}({}^6\text{Li}, {}^6\text{Li}^*){}^6\text{Li}^*$  reaction (dashed line) and up to order 18 for the  ${}^6\text{Li}({}^6\text{Li}, {}^6\text{He}){}^6\text{Be}$  reaction (solid line). Lines through the 36-MeV data are freely drawn.

things: statistical uncertainties, further nonstatistical uncertainties in the background subtraction, and the uncertainty in the efficiency corrections where applicable. An over-all 5% normalization error which affects all data equally is not included in the quoted errors. The data show diffraction patterns which shift slightly forward in angle as the bombarding energy increases from 32 to 36 MeV. We have expanded these cross sections in a series of even Legendre polynomials. The fits to data at  $E_{\text{lab}} = 32$  MeV are shown in Fig. 3, and the  $\chi^2$  of the fits as we increase the number of polynomials in the expansion are plotted in Fig. 4. The  $\chi^2/\text{degree of freedom}$  is defined as

$$\frac{1}{N-P} \sum_{i=1}^N \left( \frac{\sigma_{\text{th}}(\theta_i) - \sigma_{\text{exp}}(\theta_i)}{\Delta\sigma_{\text{exp}}(\theta_i)} \right)^2, \quad (8)$$

where  $N$  is the number of data points and  $P$  is the number of free parameters. The  $\chi^2$  goes below 1 because the errors,  $\Delta\sigma_{\text{exp}}(\theta)$ , include systematic errors as well as statistical errors.

Only even angular momenta are allowed in the  ${}^6\text{Li}({}^6\text{Li}, {}^6\text{Li}^*) {}^6\text{Li}^*$  reaction according to Bose-Einstein statistics which require that the total wave function be symmetric in the exchange of the two identical nuclei in both the incoming and outgoing channels. In the outgoing channel both the spin and isospin wave functions are necessarily symmetric and therefore the spatial wave function must also be symmetric. This means that  $L_{\text{max}}$  must be even. The  $\chi^2$  plot supports this conclusion,

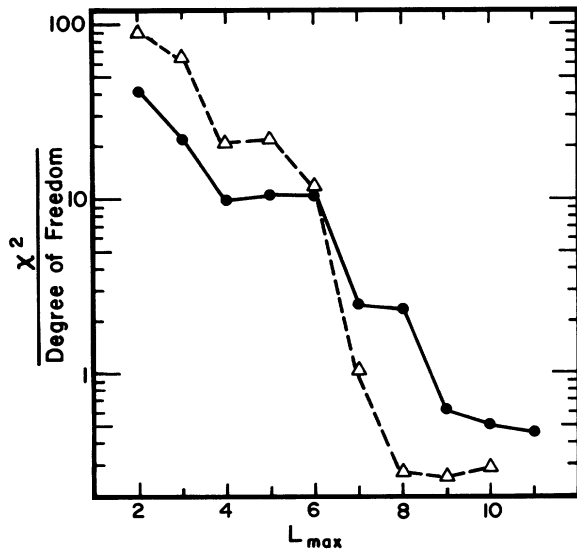


FIG. 4.  $\chi^2$  plots are shown for fits to the 32-MeV data, holding the total cross sections fixed at  $193 \mu\text{b}$  for the  ${}^6\text{Li}({}^6\text{Li}, {}^6\text{Li}^*) {}^6\text{Li}^*$  reaction and at  $158 \mu\text{b}$  for the  ${}^6\text{Li}({}^6\text{Li}, {}^6\text{He}) {}^6\text{Be}$  reaction and using the even Legendre polynomial expansion  $d\sigma_{\text{c.m.}}/d\Omega = \sum_{L=0}^{L_{\text{max}}} a_{2L} P_{2L}(\cos\theta)$ .

indicating that  $L_{\text{max}} = 8$  which corresponds to a maximum impact parameter of 5.6 fm in the ingoing channel. This distance corresponds to a grazing collision. The two orders of magnitude drop in  $\chi^2$  from  $L = 6$  to  $L = 8$  suggests that the  $L = 8$  partial wave is giving a significant contribution to the cross section. This is expected since the  ${}^6\text{Li}$  nuclei are strongly absorbed and most of the reaction is probably taking place at the surface of the nuclei. A larger  $L_{\text{max}}$  seems necessary for the  ${}^6\text{Li}({}^6\text{Li}, {}^6\text{He}) {}^6\text{Be}$  reaction and this  $L_{\text{max}}$  must also be even unless there is a significant amount of charge dependence in the reaction mechanism which allows  ${}^6\text{He}$  and  ${}^6\text{Be}$  to be in an odd relative orbital angular momentum state in the outgoing channel. Any contribution from the odd- $L$  partial waves must add incoherently with the much larger contribution from the even- $L$  partial waves (because of symmetry about  $90^\circ$ ), and theoretically it is expected that  $L_{\text{max}} = 8$  or  $10$  rather than  $L_{\text{max}} = 9$  or  $11$ . The  $\chi^2$  plot does not give a clear cutoff and all that can be said is  $L_{\text{max}} \geq 9$ .

The total cross sections at 32 MeV are obtained from the least-squares polynomial fit and are  $193 \pm 12 \mu\text{b}$  for the  ${}^6\text{Li}({}^6\text{Li}, {}^6\text{Li}^*) {}^6\text{Li}^*$  reaction and  $158 \pm 10 \mu\text{b}$  for the  ${}^6\text{Li}({}^6\text{Li}, {}^6\text{He}) {}^6\text{Be}$  reaction.

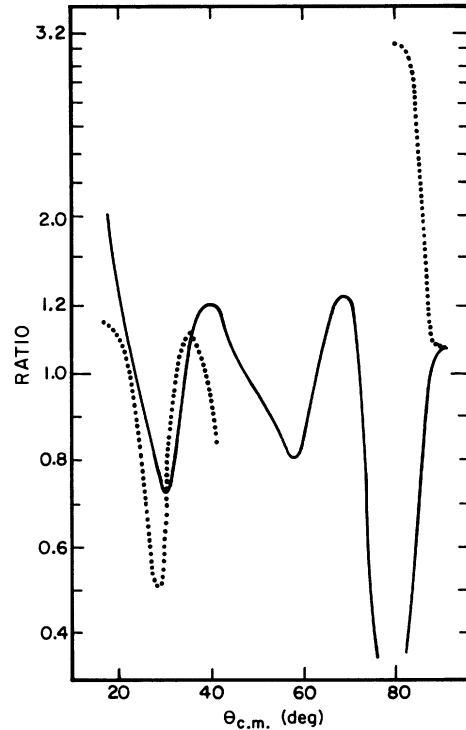


FIG. 5. The ratio of the differential cross sections  $\sigma({}^6\text{Li}^*)/\sigma({}^6\text{He})$  at  $E_{\text{lab}} = 32$  MeV (solid line) and at  $E_{\text{lab}} = 36$  MeV (dotted line) are shown corresponding to the lines drawn through the data in Fig. 3. The solid line is a result of a least-squares Legendre polynomial fit to the data at 32 MeV.

The errors give the range of possible values for the total cross section such that the  $\chi^2$  of the fit is within 50% of its minimum. In determining these errors it is assumed that the maximum-order polynomial in the  ${}^6\text{Li}({}^6\text{Li}, {}^6\text{Li}^*){}^6\text{Li}^*$  and  ${}^6\text{Li}({}^6\text{Li}, {}^6\text{He}){}^6\text{Be}$  angular distributions is 16 and 18, respectively. Therefore the error in the total cross section is underestimated if higher-order polynomials are needed to fit the unmeasured cross section forward of  $17^\circ$ .

The ratio of the total cross sections  $\sigma({}^6\text{Li}^*)/\sigma({}^6\text{Be})$  at 32 MeV is  $1.22 \pm 0.14$  with most of the error resulting from the unmeasured cross section at forward angles. The variation of the ratio of the cross sections with angle is plotted in Fig. 5. The ratio plotted against center-of-mass angle must involve knowledge of the shape of the angular distributions because the simultaneous measurement of the cross sections of both reactions at the same laboratory angle does not correspond to the same center-of-mass angle for each reaction. The Legendre polynomial fits to the cross sections involve the full shape of the angular distributions and therefore are used to determine the ratio of the cross sections at 32 MeV shown in Fig. 5. The ratio at 36 MeV is much more subjective involving the ratio of freely drawn lines through the data.

The deviations of the ratio from unity are large both in magnitude and relative to the errors involved (Fig. 3 shows the errors), especially near  $20^\circ$  and  $80^\circ$  at 32 MeV and near  $30^\circ$  and  $80^\circ$  at 36 MeV. Therefore it is clear that charge-dependent effects are important. The ratio has a strong oscillatory angular dependence which is a result of the  ${}^6\text{Li}({}^6\text{Li}, {}^6\text{He}){}^6\text{Be}$  angular distribution being shifted several degrees backwards from the  ${}^6\text{Li}({}^6\text{Li}, {}^6\text{Li}^*){}^6\text{Li}^*$  angular distribution. The ratio of the cross sections at  $80^\circ$  is very energy-dependent, changing by a factor of 16 as the center-of-mass energy changes by 2 MeV from 16 to 18 MeV. This strong energy dependence in the ratio is occurring where the cross section has a deep minimum. Here the ratio is likely to be sensitive to small contributions from various reaction mechanisms, especially if there is destructive interference at  $80^\circ$ .

Excitation functions also have been measured for both reactions at the same laboratory angle corresponding to the center-of-mass angles:  $\theta_{\text{Li}} = \pi - \theta_{\text{He}} \approx 88^\circ$ . This angle was chosen because the cross sections are necessarily symmetric about  $90^\circ$ , and therefore the ratio of the cross sections at the same center-of-mass angle is directly obtainable from each measurement independent of any angular dependence in the cross sections. The excitation functions and their ratio are shown in Fig. 6 along with earlier data by

Nagatani *et al.*<sup>2</sup> which have been renormalized upwards by a factor of 1.6 so that their backward-angle elastic cross sections agree with the elastic cross sections of Fortune, Morrison, and Siemsen.<sup>9</sup> The cross sections are smoothly varying with energy.

Our data are consistent with the earlier published data on the  ${}^6\text{Li}({}^6\text{Li}, {}^6\text{Li}^*){}^6\text{Li}^*$  reaction at 32 MeV (after renormalization) except at the very forward angles where our data indicate considerably larger cross sections. The disagreement is presumably a result of multiple scattering effects which were not included in the efficiency corrections of Ref. 2.

### SUMMARY

A reasonable amount of data has been collected on the  ${}^6\text{Li}({}^6\text{Li}, {}^6\text{Li}^*){}^6\text{Li}^*$  and  ${}^6\text{Li}({}^6\text{Li}, {}^6\text{He}){}^6\text{Be}$  reactions, and a comparison of the cross sections for the two reactions has been made. The experimental ratio of the cross sections deviates significantly from unity and shows large variations with angle and energy. The data on the ratio not only will be of value for determining the extent to which the reaction mechanism is quasielastic but also may be of value for studying differences in the wave functions of the  $T=1$  isomultiplet; the

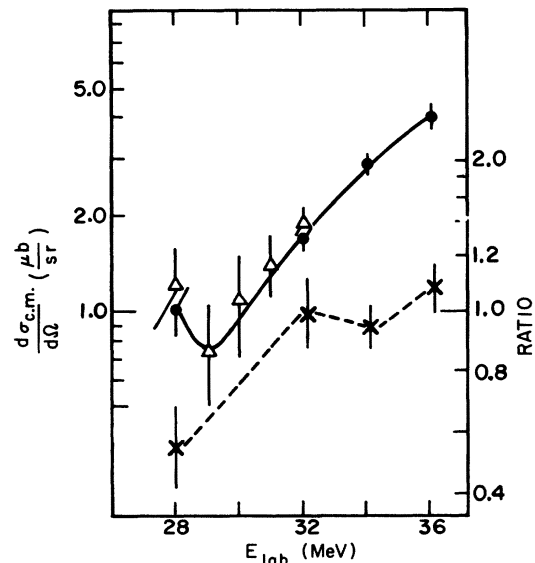


FIG. 6. The excitation function of the  ${}^6\text{Li}({}^6\text{Li}, {}^6\text{Li}^*){}^6\text{Li}^*$  reaction at  $90^\circ$  in the center of mass taken from Ref. 2 (triangles) and the present data at  $88^\circ$  c.m. (solid circles) are shown with a freely drawn line through the data. The data from Ref. 2 has been renormalized upwards by a factor of 1.6 (see text) and the scale is on the left. The ratio of the differential cross sections  ${}^6\text{Li}({}^6\text{Li}, {}^6\text{Li}^*)\text{-}{}^6\text{Li}^*/{}^6\text{Li}({}^6\text{Li}, {}^6\text{He}){}^6\text{Be}$  at  $88^\circ$  c.m. (x) also is shown with a dotted line connecting the data points and the scale is on the right.

${}^6\text{He}$  ground state,  ${}^6\text{Li}^*(3.56 \text{ MeV})$ , and the  ${}^6\text{Be}$  ground state. In an attempt to study these and other questions a partially microscopic DWBA

calculation has been made, compared to the experimental results, and is presented in a subsequent report.<sup>5</sup>

\*Work supported in part by the U. S. Atomic Energy Commission.

†Present address: Argonne National Laboratory, Argonne, Illinois 60439.

‡Present address: Varian Physics Laboratory, Stanford University, Stanford, California 94305.

<sup>1</sup>V. I. Chuev, V. V. Davydov, V. I. Manko, B. G.

Novatsky, S. B. Sakuta, and D. N. Stepanov, *Phys. Lett.* **31B**, 624 (1970).

<sup>2</sup>K. Nagatani, D. P. Boyd, P. F. Donovan, E. Beardsworth, and P. A. Assimakopoulos, *Phys. Rev. Lett.* **24**, 675 (1970).

<sup>3</sup>C. F. Clement and S. M. Perez, *Nucl. Phys.* **A195**, 561 (1972).

<sup>4</sup>A. N. Boyarkina, *Izv. Akad. Nauk SSSR Ser. Fiz.* **28**, 337 (1964) [transl.: *Bull. Acad. Sci. USSR Phys. Ser.*

**28**, 255 (1964)].

<sup>5</sup>W. R. Wharton, following paper, *Phys. Rev. C* **9**, 164 (1974).

<sup>6</sup>W. K. Dawson, D. W. Storm, and H. H. Wieman, private communication.

<sup>7</sup>W. R. Wharton and H. Wieman, University of Washington Annual Report No., 1971 (unpublished) p. 69.

<sup>8</sup>L. C. Northcliffe and R. F. Schilling, *Nucl. Data* **A7**, 233 (1970).

<sup>9</sup>H. T. Fortune, G. C. Morrison, and R. H. Siemssen, *Phys. Rev. C* **3**, 2116 (1971).

<sup>10</sup>J. Heagney, private communication.

<sup>11</sup>J. B. Marion and B. A. Zimmerman, *Nucl. Instrum. Methods* **51**, 93 (1967).

<sup>12</sup>W. R. Wharton, Ph.D. thesis, University of Washington, 1972 (unpublished).